

Study of the nitrogen diffusion mechanism in R_2Fe_{17}

Y. D. Zhang, J. I. Budnick, and W. A. Hines

Department of Physics and Institute of Materials Science, University of Connecticut, Storrs, Connecticut 06269

D. P. Yang

Department of Physics, College of the Holy Cross, Worcester, Massachusetts 01610

Previously, nuclear magnetic resonance experiments and diffusion calculations have indicated that the distribution of nitrogen atoms in a $Y_2Fe_{17}N_x$ particle with intermediate N content is characterized by a nitrated region and an unnitrated region. In order to *directly* detect this two-region configuration, x-ray diffraction experiments have been carried out on systematically ground nitrogenated samples. Furthermore, x-ray diffraction and ^{89}Y nuclear magnetic resonance on vacuum-annealed samples show that the two-region configuration is stable, and that the nitrogen atoms do not diffuse further into the particle. Thermal conductivity detection measurements indicate that only 5% of the inserted N atoms can be released by vacuum annealing at the nitrogenation temperature. © 1996 American Institute of Physics. [S0021-8979(96)36908-3]

I. INTRODUCTION

It is now well known that nitrogen insertion into rare-earth+Fe intermetallics, such as R_2Fe_{17} , produces materials with significantly improved magnetic properties, namely, the Curie temperature, magnetocrystalline anisotropy, and Fe magnetic moment.^{1,2} A thorough understanding of the nitrogen diffusion process in the host lattice is important for determining the optimal nitrogenation conditions that will result in homogeneous and stable magnetic properties.

Recently, it has been shown that the distribution of nitrogen in a $Y_2Fe_{17}N_x$ particle with intermediate N content is characterized by a nitrated/unnitrated configuration.^{3,4} In a simple case, this can be a shell/core structure. In the nitrated outer shell, all of the *accessible* interstitial sites are occupied by N atoms, and in the inner core, the host lattice is almost devoid of N atoms. These two regions share a thin interface, and the nitrogen atoms in a spherical $Y_2Fe_{17}N_x$ particle have an overall steplike radial distribution. The experimental evidence for this configuration came from ^{89}Y nuclear magnetic resonance (NMR) spectra, which showed that, across the entire range of nitrogen content ($0.6 \leq x \leq 2.8$), there are predominantly two types of Y-N coordination, namely, yttrium with two nitrogen atoms as nearest neighbors (Y+2N), and yttrium with no nitrogen atom as a nearest neighbor (Y+0N).³ This implies that in the nitrated region, two of the three octahedral sites are occupied, and in the unnitrated region, the octahedral sites are empty. The process of nitrogenation results in the growth of the nitrated outer shell at the expense of the unnitrated inner core, with the nitrated region maintaining a Y+2N coordination. The Y+2N coordination for the nitrated region in $Y_2Fe_{17}N_x$ has also been determined from neutron diffraction.⁵ The nitrated/unnitrated configuration was observed in $Nd_2Fe_{17}N_x$ using neutron diffraction,⁶ and in $Pr_2Fe_{17}N_x$ using Mössbauer spectroscopy.⁷ This step-like distribution was studied in several systems, such as $Nd_2Fe_{17}N_{2,3}$, where a sharp interface with thickness of only 1 μm was detected using electron microprobe analysis.⁸

In this article, additional experimental evidence supporting the above nitrated/unnitrated configuration is presented. In order to detect the two regions *directly*, x-ray diffraction

patterns have been obtained from $Y_2Fe_{17}N_x$ samples after successive stages of grinding, and they confirm that the nitrogen distribution is not continuous and the inner core is not nitrated. The stability of the two-region configuration is studied by both x-ray diffraction and ^{89}Y NMR which show essentially no change for a nitrogenated sample upon vacuum annealing. Finally, the number of mobile N atoms is measured directly using thermal conductivity detection (TCD) in an outgassing process, and found to be approximately 5% of the total N content.

II. EXPERIMENTAL APPARATUS AND PROCEDURE

The parent Y_2Fe_{17} ingot, made by arc melting, was homogenized, powdered, and sieved to give particle diameters from 32 to 37 μm . The powder was annealed at 900 °C in an Ar atmosphere for 5 days before nitrogenation, which was performed at 480 °C under an ultrahigh purity (99.999%) N_2 flow. $Y_2Fe_{17}N_x$ samples with different N content ($0.3 \leq x \leq 2.8$) were obtained by varying the nitrogenation time from 0.5 to 18 h. Further vacuum annealing of the $Y_2Fe_{17}N_{1.7}$ sample was performed at 480 °C for 12 h using the same apparatus.

X-ray diffraction patterns were obtained on a Norelco diffractometer using Cu $K\alpha$ radiation. Nitrogen outgassing experiments were carried out on a temperature-programmed desorption apparatus.⁹ A tube containing the $Y_2Fe_{17}N_{2.8}$ sample was subject to a flow of helium gas at a fixed rate. The desorbed nitrogen effluent was detected with a thermal conductivity detector. Spin-echo NMR measurements were made at 4.2 K, in zero external field, using a 120°–120° pulse sequence. The pulsed NMR apparatus, signal coil arrangement, calibration, and data taking procedure have been described in detail elsewhere.¹⁰

III. RESULTS AND ANALYSIS

Figure 1 compares the x-ray diffraction patterns of three powder samples: (a) the parent sample Y_2Fe_{17} ; (b) the “completely” nitrated sample $Y_2Fe_{17}N_{2.8}$; and (c) the intermediate N content sample $Y_2Fe_{17}N_{1.7}$. In Fig. 1(a), a single hexagonal

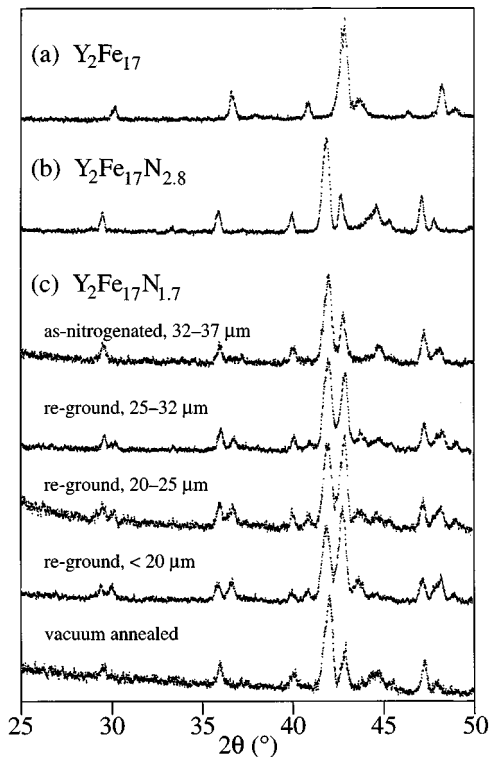


FIG. 1. X-ray diffraction patterns from (a) the parent sample Y_2Fe_{17} , (b) the “completely” nitrided sample $Y_2Fe_{17}N_{2.8}$, and (c) an intermediate N content sample $Y_2Fe_{17}N_{1.7}$. Two sets of Bragg peaks are visible in the reground $Y_2Fe_{17}N_{1.7}$ samples, showing the nitrided outer shell and the unnitrided inner core. Also, there is no significant structural differences between the as-nitrogenated and vacuum-annealed samples of $Y_2Fe_{17}N_{1.7}$.

Y_2Fe_{17} phase with no bcc α -Fe is identified for the parent sample. For the $Y_2Fe_{17}N_{2.8}$ sample [Fig. 1(b)], the same structure as the parent sample is identified except that all of the Bragg peaks are shifted to lower angles due to volume expansion. Also, a small amount of α -Fe precipitation is present. In Fig. 1(c), the Bragg peaks from the as-nitrogenated $Y_2Fe_{17}N_{1.7}$ sample are *not* located, commensurate with its intermediate N content, between the diffraction peaks in Figs. 1(a) and 1(b). Rather, they are located essentially at the same angles as those in Fig. 1(b), indicating a near complete nitrogenation of the surface region of the particle since the penetration depth for x rays in $Y_2Fe_{17}N_x$ is less than 5 μm . In order to expose the interior of the particles to the x rays, the $Y_2Fe_{17}N_{1.7}$ sample was ground in stages to obtain three samples with particle diameters of 25–32, 20–25, and <20 μm . As shown in Fig. 1(c), the three ground $Y_2Fe_{17}N_{1.7}$ samples have an extra set of Bragg peaks that correspond to the unnitrided parent sample Y_2Fe_{17} shown in Fig. 1(a). Furthermore, the smaller the particle size, the larger the peaks in the second set, showing directly more of the unnitrided inner core. A careful inspection of the x-ray patterns shows that the 2θ value of a peak in the unnitrided phase for a sample with intermediate N content is a little smaller than that for the parent Y_2Fe_{17} sample, and the 2θ value of a peak in the nitrided phase for a sample with intermediate N content is a little larger than that for the completely nitrided sample. The result can be explained by lattice

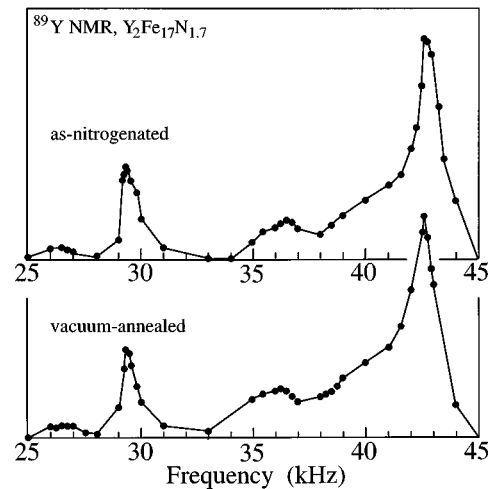


FIG. 2. ^{89}Y NMR spectra from as-nitrogenated and vacuum-annealed samples of $Y_2Fe_{17}N_{1.7}$, showing no significant structural changes after vacuum annealing at the nitrogenation temperature.

strain since the two phases coexist in the sample particle. Lattice strain will result in the phase with smaller lattice constants being stretched, and the phase with large lattice constants being compressed.

As discussed below, the reason for the formation of such a two-region distribution is a strong chemical bond between a nitrogen atom in an interstitial octahedral site and the surrounding environment in the lattice. If there is such a trapping of the N atoms at the nitrogenation temperature (480 °C), then the distribution should be stable at the same temperature. The nitrogenated samples have been vacuum annealed, and x-ray diffraction and ^{89}Y NMR have been used to detect any changes in the N distribution. Both the x-ray diffraction pattern [Fig. 1(c)] and the NMR spectrum (Fig. 2) of the vacuum-annealed $Y_2Fe_{17}N_{1.7}$ sample remain unchanged from the as-nitrogenated sample. These experiments verify the stability of the two-region distribution, and therefore, the strong N-lattice bonding.

Finally, the number of mobile N atoms in the $Y_2Fe_{17}N_{2.8}$ sample was analyzed quantitatively in an outgassing experiment using thermal conductivity detection (TCD). The TCD signal voltage which was recorded as the temperature of the sample increased showed three peaks, each corresponding to an effluence of N atoms from the sample. A first peak near 120 °C was attributed to those N atoms adsorbed on the surface, which accounted for about 1% of the total N content. A second peak near 380 °C was attributed to the outgassing of the mobile N atoms inside the sample. Finally, a third peak, or sudden increase in the TCD signal, above 600 °C was attributed to nitrogen release during the phase decomposition into YN and α -Fe. In order to obtain a reasonable estimate for the amount of nitrogen release associated with the second peak, the TCD experiment was repeated with the temperature scan programmed to stop rising at 460 °C (above the second peak but below the temperature of phase decomposition). During a 15 min period at a constant temperature of 460 °C, the mobile N atoms were completely evacuated from the

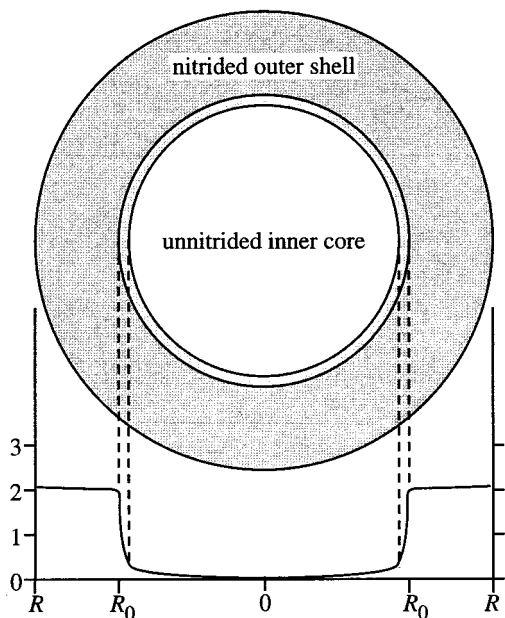


FIG. 3. Schematic diagram showing the nitrogen distribution in a spherical particle. The horizontal scale represents the radial direction across the particle, and the vertical scale represents the N concentration in nitrogen atoms per unit cell in $Y_2Fe_{17}N_x$.

sample. Integration of the second peak and comparison with a standard calibration curve showed that about 5% of the total N content can be released. If none of N atoms were trapped in the interstitial sites, then during the vacuum-annealing process the N atoms would either diffuse further towards the interior of the particle or leave the particle through its surface. The first possibility would have caused changes in the x-ray diffraction pattern and NMR spectrum, whereas the second possibility would have been detected in the outgassing experiment. The experiments rule out both of these scenarios for the majority of N atoms in the $Y_2Fe_{17}N_x$ system.

IV. DISCUSSION AND CONCLUSIONS

To date, two different models have been proposed for describing the nitrogen distribution in $R_2Fe_{17}N_x$. One is based on a simple diffusion mechanism that results in a continuous solid solution distribution (CSSD) with a smooth concentration gradient.^{11,12} The second model considers a chemical reaction diffusion process with two types of N atoms that leads to a steplike radial distribution with a nitrided shell and an unnitrided core (see Fig. 3).⁴ One type of nitrogen atom is characterized by its immobility once the atom enters an accessible octahedral site (trapped type, or *t*-type), and the other has a relatively large diffusion constant (free-type, or *f*-type). It is reasonable to believe that the *f*-type atoms are located in the tetrahedral interstitial sites as reported in a previous ¹⁴N NMR study on both hexagonal and rhombohedral $Y_2Fe_{17}N_x$.¹³ The *t*-type atoms are immobilized because of a strong chemical bond with the lattice. The *f*-type atoms can diffuse easily only in the region where all the “traps” are filled, otherwise an *f*-type atom would fall

into an octahedral site and convert itself into a *t*-type atom. In the outer shell, therefore, all accessible interstitial octahedral sites are occupied by *t*-type N atoms, and a relatively small number of *f*-type atoms “ride” on the nitrided region and diffuse towards the interface where octahedral interstitial sites are available. Once an *f*-type atom reaches the interface, it is immediately trapped and converts to a *t*-type atom, leaving a sharp boundary between the nitrided outer region and an unnitrided inner one. Through this process, the interface advances towards the center of the particle, and the nitrogen content in the sample increases with nitrogenation time. If the nitrogenation is terminated, either by removing the nitrogen gas source or by reducing the temperature, then the interface ceases to move and the steplike distribution is preserved. In the case that the trapping has a relatively deep potential well, this two-region configuration is stable. The chemical reaction diffusion process with two types of N atoms described above has been treated theoretically in a previous work which calculates the radial dependence of the nitrogen distribution (see Fig. 3).⁴ In addition, this model explains the abnormally small (apparent) diffusion frequency factor which characterizes these newly developed R_2Fe_{17} nitrides.⁴

Finally, the “nominal” nitrogen content is usually obtained by weighing the sample before and after nitrogenation; consequently, there are errors as not all the N atoms absorbed into the entire sample are coordinated with the Y atoms in the 2:17 phase. Also some of the weight gain of the sample may be due to factors other than N absorption. This may offer an explanation as to why different studies have reported different N content values, while the corresponding lattice expansion and magnetic properties were not so different. A detailed analysis of the difference between the N content measured gravimetrically and the Y–N coordination measured by NMR has been published previously.¹⁴

ACKNOWLEDGMENT

This work was supported by NSF Grant No. DMR9319367.

- ¹J. M. D. Coey and H. Sun, *J. Magn. Magn. Mater.* **87**, L251 (1990).
- ²K. H. J. Buschow, *J. Alloys Comp.* **193**, 223 (1993).
- ³Y. D. Zhang, J. I. Budnick, D. P. Yang, G. W. Fernando, W. A. Hines, T. D. Xiao, and T. Manzur, *Phys. Rev. B* **51**, 12091 (1995).
- ⁴Y. D. Zhang, J. I. Budnick, W. A. Hines, and D. P. Yang, *Appl. Phys. Lett.* **67**, 208 (1995).
- ⁵S. S. Jaswal, W. B. Yelon, G. C. Hadjipanayis, Y. Z. Wang, and D. J. Sellmyer, *Phys. Rev. Lett.* **67**, 644 (1991).
- ⁶O. Isnard, J. L. Soubeyroux, S. Miraglia, D. Fruchart, L. M. Garcia, and J. Bartolomé, *Physica B* **180–181**, 624 (1992).
- ⁷A. I. C. Persiano, J. D. Ardisson, F. A. Batista, C. C. Colucci, and S. Gama, *J. Magn. Magn. Mater.* **136**, 149 (1994).
- ⁸C. C. Colucci, S. Gama, C. A. Ribeiro, and L. P. Cardoso, *J. Appl. Phys.* **75**, 6003 (1994).
- ⁹W. Q. Xu, S. L. Suib, and C. L. O’Young, *J. Catal.* **144**, 285 (1993).
- ¹⁰Y. D. Zhang, W. A. Hines, J. I. Budnick, M. Choi, F. H. Sanchez, and R. Hasegawa, *J. Magn. Magn. Mater.* **61**, 162 (1986).
- ¹¹J. M. D. Coey, R. A. Skomski, and S. Wirth, *IEEE Trans. Magn.* **28**, 2332 (1992).
- ¹²R. Skomski and J. M. D. Coey, *J. Appl. Phys.* **73**, 7602 (1993).
- ¹³Y. D. Zhang, J. I. Budnick, W. A. Hines, N. X. Shen, T. D. Xiao, and T. Manzur, *J. Magn. Magn. Mater.* **145**, L11 (1995).
- ¹⁴Y. D. Zhang *et al.*, *Scr. Metall. Mater.* **33**, 1817 (1995).